NATIONAL ADVISORY COMMITTEE FOR AERONAUTICS

WARTIME REPORT

ORIGINALLY ISSUED

February 1943 as
Memorandum Report

HIGH-SPEED WIND-TUNNEL TESTS OF A 1/14-SCALE MODEL OF A FOUR-ENGINE CARGO AIRPLANE

By William T. Hamilton

Ames Aeronautical Laboratory
Moffett Field, California

WASHINGTON

NATIONAL ADVISORY COMMITTEE FOR AERONAUTICS

MEMORANDUM REPORT

for the

Air Materiel Command, U. S. Army Air Forces

HIGH-SPEED WIND-TUNNEL TESTS OF A 1/14-SCALE MODEL OF A FOUR-ENGINE CARGO AIRPLANE

By William T. Hamilton

SUMMARY

This report presents results of tests on a 1/14-scale model of a four-engine cargo airplane, which was tested in the 16-foot high-speed wind tunnel. The high-speed characteristics of this airplane, particularly the longitudinal stability and control in dives were investigated.

The test results indicated no important changes in longitudinal stability or controllability until the speed exceeded the predicted maximum level-flight speed by more than 38 percent. Above this speed, large changes occurred in the stability and lift coefficient for balance.

INTRODUCTION

At the request of the Army Air Forces, a 1/14-scale model of a cargo airplane was tested in the 16-foot high-speed wind tunnel at the Ames Aeronautical Laboratory of the National Advisory Committee for Aeronautics. The airplane is a four-engine low-wing monoplane.

The purpose of the tests was to investigate the high-speed characteristics of this airplane, particularly the longitudinal stability and control in dives.

APPARATUS

Model

A three-view drawing of the model is shown in figure 1 and pertinent information is given in table I. Figure 2 shows the complete model installed in the 16-foot wind tunnel. The outboard nacelles could not be completely removed because they housed the forward support trunnions, hence their usual cowled noses and spinners were replaced by smooth faired noses (fig.3) for certain basic tests.

The wing was built of mahogany screwed to a hollow steel spar of welded construction. The fuselage was made of solid mahogany and bolted to the wing. The nacelles were made of solid birch and were screwed to the wing. The tail was made of aluminum alloy and was bolted to the fuselage. The elevators were held in place by steel brackets. The fillets were made of "cerro-bend" metal.

As originally tested, the model fluttered. This condition was remedied by adding approximately 50 pounds of lead shot in the nose of the fuselage.

Wind Tunnel

The tests were conducted in the Ames 16-foot-diameter, high-speed, single-return wind tunnel. Forces and moments were measured by the automatic balancing and recording scales.

RESULTS

The results are reduced to the usual lift, drag and moment coefficients and presented as functions of M, α, and α_u.

where

M Mach number $\left(\frac{\text{speed of air stream}}{\text{speed of sound}}\right)$

α angle of attack of the fuselage reference line, corrected for the tunnel-wall effects as given in the equation for $\Delta\alpha$

α_u geometric angle of attack of the fuselage reference line

Pitching moments are given about the center of gravity as located in figure 1.

The following tunnel-wall corrections were applied to the test results (reference 1):

$$\Delta\alpha = 0.310\ C_L$$

$$\Delta C_D = 0.0054\ C_L^2$$

$$\Delta C_m = 0.0057\ C_L \quad \text{(tail-on runs only)}$$

Approximate lift, drag, and pitching-moment tares were obtained with the model removed leaving the struts with fairings on their upper ends, as in figure 4. These tares are shown in figure 5. Since no corrections for buoyancy, stream inclination, or interference have been applied to the drag data, they should be used for comparative purposes only. The pitching moments have been corrected for the downflow of the air stream at the tail position of the model (fig. 6). This downflow was measured with the model removed.

DISCUSSION OF RESULTS

Longitudinal Stability

The characteristics of the model in various stages of completeness are shown in figures 7, 8, and 9. Figures 7 and 8 indicate that the tail-off instability increased at Mach numbers above 0.675. Figure 9, which shows the characteristics of the complete model, indicates no appreciable change in pitching moment or static longitudinal stability through the range of Mach numbers from 0.3 to 0.5. As the Mach number increased from 0.5 to 0.65, the stability decreased at negative lift coefficients, but remained about the same at positive lift coefficients. About 0.65 Mach number, the stability increased and a large change in the lift coefficient for balance occurred. The increase in stability appeared first at the higher lift coefficients, as indicated by the breaks in the moment curves of figure 9(d). Because of the increase in stability and the change in lift coefficient for balance, a greater increment of pitching moment is required of the elevator in order to control the airplane. At lift coefficients corresponding to level flight this increase in stability appeared at speeds ranging from 460 miles per hour at 29,000 feet altitude to 515 miles per hour at sea level. This result indicates a considerable margin of safety over the predicted maximum speeds in level flight of 247 miles per hour at 29,000 feet

altitude and 301 miles per hour at sea level. This margin is least at 18,000 feet altitude, where it is 38 percent.

Figure 10(a) indicates that the wing-fuselage fillet, the inboard nacelles, and the outboard nacelle cowls had no appreciable effect on the stability for the tail-off condition of the model. With the tail on the model, both the inboard nacelles and wing-fuselage fillets added negative increments of pitching moment and increased the stability slightly at speeds below the critical Mach number (as indicated by the start of the precipitous increase of the drag) as shown by figures 10(b) and 10(c). At the higher lift coefficients, the addition of the fillets increased the value of Mach number at which the break in the moment curves occurred.

The elevator effectiveness, as indicated by the effect of the elevator on the pitching moment, remained essentially constant with speed for Mach numbers up to 0.725 and small lift coefficients, but decreased at Mach numbers greater than 0.6 for lift coefficients of 0.3 or more (fig. 11). Though the elevator was capable of producing changes in the pitching moment at speeds above the critical, the increased stability rendered it less capable of controlling the attitude and lift coefficient at these speeds.

Lift

In general, the lift coefficient at constant angle of attack increased with speed until the critical speed was reached (figs. 7(c), 8(c), 9(c)). At the higher angles, the lift coefficients fell off before the critical speed was reached. As the critical speed was exceeded the lift decreased rapidly. All of these effects are considered normal. The addition of the wing-fuselage fillets increased the slope of the lift curve slightly and increased the critical speed for large angles of attack (fig. 12(c)), thereby giving higher lifts at high speeds. The addition of the inboard nacelles decreased the lift coefficient, at constant angle of attack, by a small amount.

Drag

The drag coefficient increased only slightly with speed until the critical speed was reached. Figures 12(a), 12(b), and 12(c), show the drag of the model in various stages of completeness. Figure 12(b) indicates that at a Mach number of 0.45 and a lift coefficient of 0.3 (a representative flight condition), the

increments of drag coefficient added by the separate addition of the component parts were as follows:

Fillets	−0.0016
Inboard nacelles	0.0012
Tail	0.0032

The 0.0032 increment of drag coefficient due to the tail was measured with the inboard nacelles removed from the model. With the inboard nacelles in place, the increment of drag coefficient due to the tail was 0.0051, an increase of 0.0019.

At small lift coefficient, the wing--fuselage fillets had little or no effect on the critical speed but, at the higher lift coefficients, the critical speed was increased by the addition of the fillets (fig. 11(c)). The addition of the inboard nacelles reduced the critical Mach number approximately 0.02.

CONCLUSIONS

1. The test results indicated that the longitudinal stability and control remained normal until speeds at least 38 percent above the maximum predicted level-flight speeds had been reached.

2. The elevator effectiveness at lift coefficients of zero and 0.1 was maintained up to a Mach number of 0.725. This Mach number was considerably higher than the critical Mach number. However, the elevator effectiveness was less at Mach numbers above 0.6 for lift coefficients greater than 0.1. The increased stability and large changes in lift coefficient for balance at speeds above the critical rendered the elevator less capable of controlling the attitude and lift coefficient at these speeds.

3. The inboard nacelles caused the drag coefficient of the tail to increase from 0.0032 to 0.0051 at a lift coefficient of 0.3, and at a Mach number of 0.45 (a representative flight).

Ames Aeronautical Laboratory,
National Advisory Committee for Aeronautics,
Moffett Field, Calif.

REFERENCE

1. Silverstein, Abe, and White, James A.: Wind-Tunnel Interference with Particular Reference to Off-Center Positions of the Wing and to the Downwash at the Tail. NACA Rep. No. 547, 1935.

TABLE I.- DIMENSIONS

NATIONAL ADVISORY
COMMITTEE FOR AERONAUTICS

ITEM	1/14 SCALE MODEL	AIRPLANE
WING:		
Area	8.43 sq ft	1652.28 sq ft
Root section	NACA 23018	
Root chord	15.714 in.	13.333 ft
Root chord incidence	+3°	
Tip section	NACA 4412	
Tip chord	7.286 in.	8.500 ft
Tip chord incidence	+1°	
Span	105.43 in.	123.0 ft
Dihedral	7°-36'-38.2"	
Aspect ratio	9.16	
Mean aerodynamic chord	12.571 in.	14.67 ft
Tail length (c.g. to elev. hinge line)	46.39 in.	54.12 ft
HORIZONTAL TAIL:		
Area	2.39 sq ft	468.44 sq ft
Span	42.86 in.	50.00 ft
Root section	inverted modified NACA 23013	
Tip section	inverted modified NACA 23010	
Incidence	+0.45°	
ELEVATOR:		
Area (aft of H)	0.57 sq ft	111.72 sq ft
Percent total horiz. tail area	23.8 percent	
Span (excluding cut-out)	16.28 in.	18.99 ft
TOTAL VERTICAL SURFACE:		
Area	1.23 sq ft	241.08 sq ft
OUTB'D VERT. SURFACE (each):		
Area	0.46 sq ft	90.16 sq ft
Wing loading	---	43.6 #/sq ft

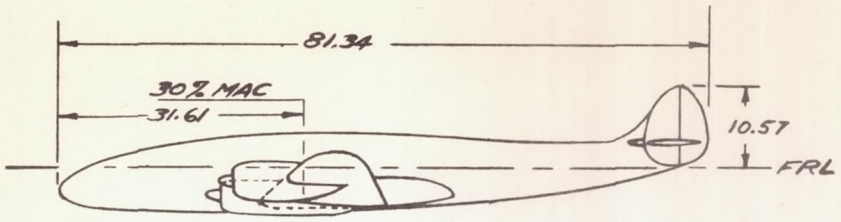

SIDE VIEW

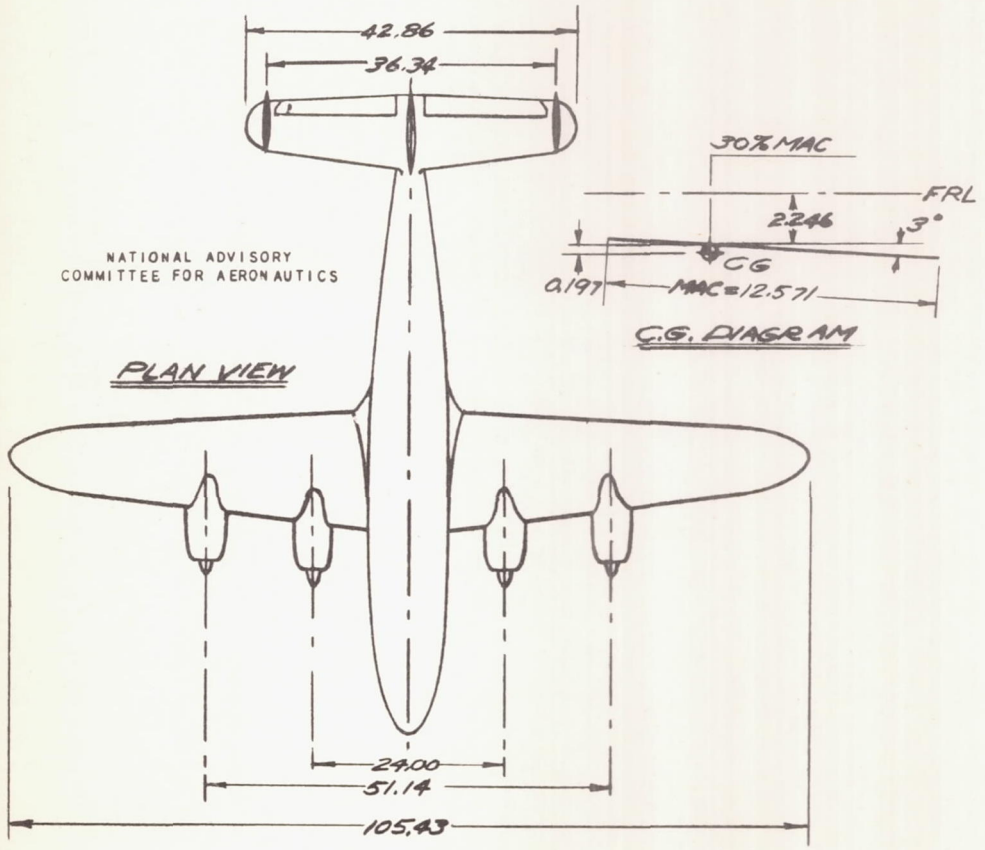

PLAN VIEW

C.G. DIAGRAM

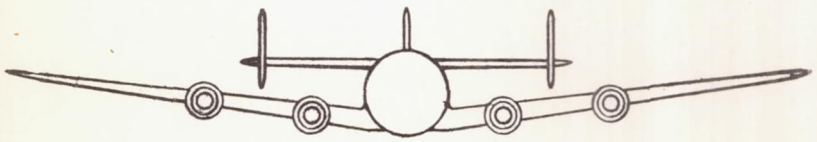

FRONT VIEW

MODEL DIMENSIONS IN INCHES

FIGURE 1.- THE $\frac{1}{14}$-SCALE MODEL CARGO AIRPLANE.

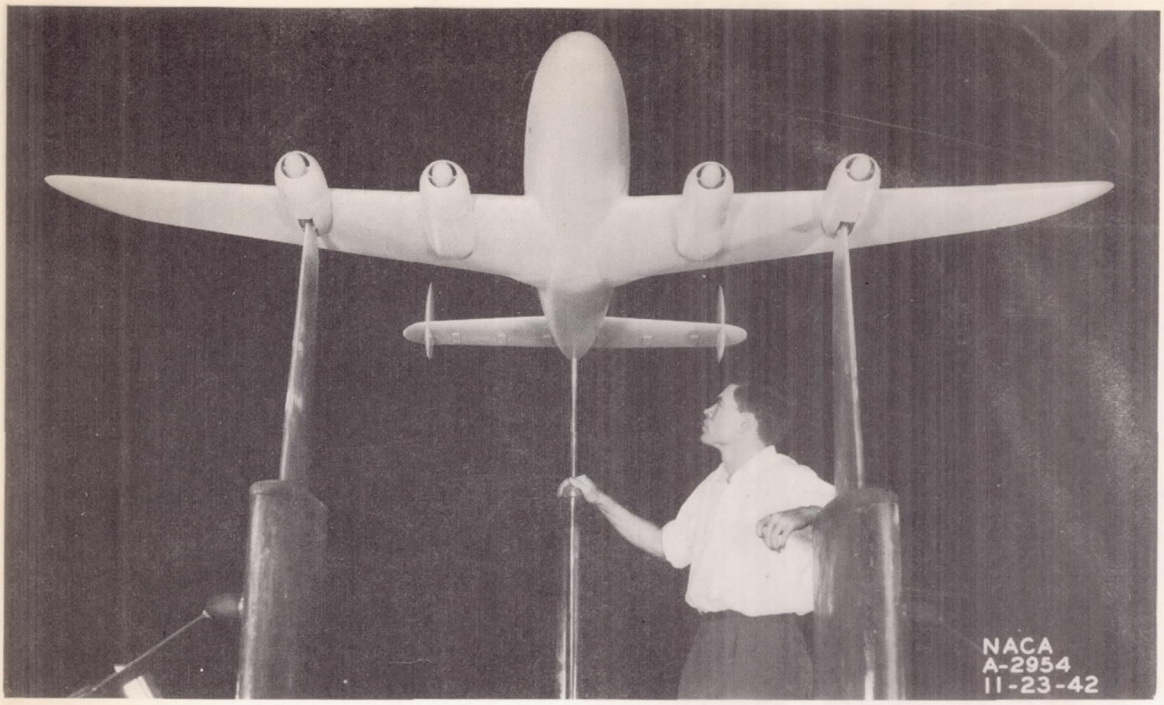

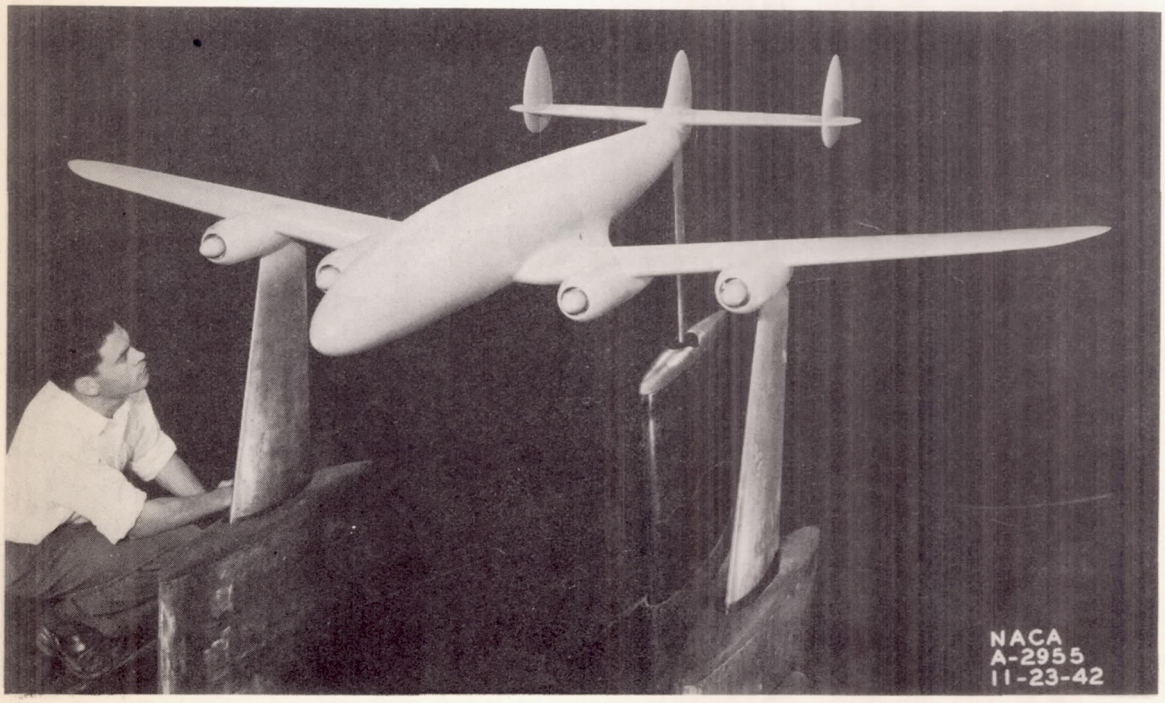

Figure 2.- The model mounted in the 16-foot wind tunnel.

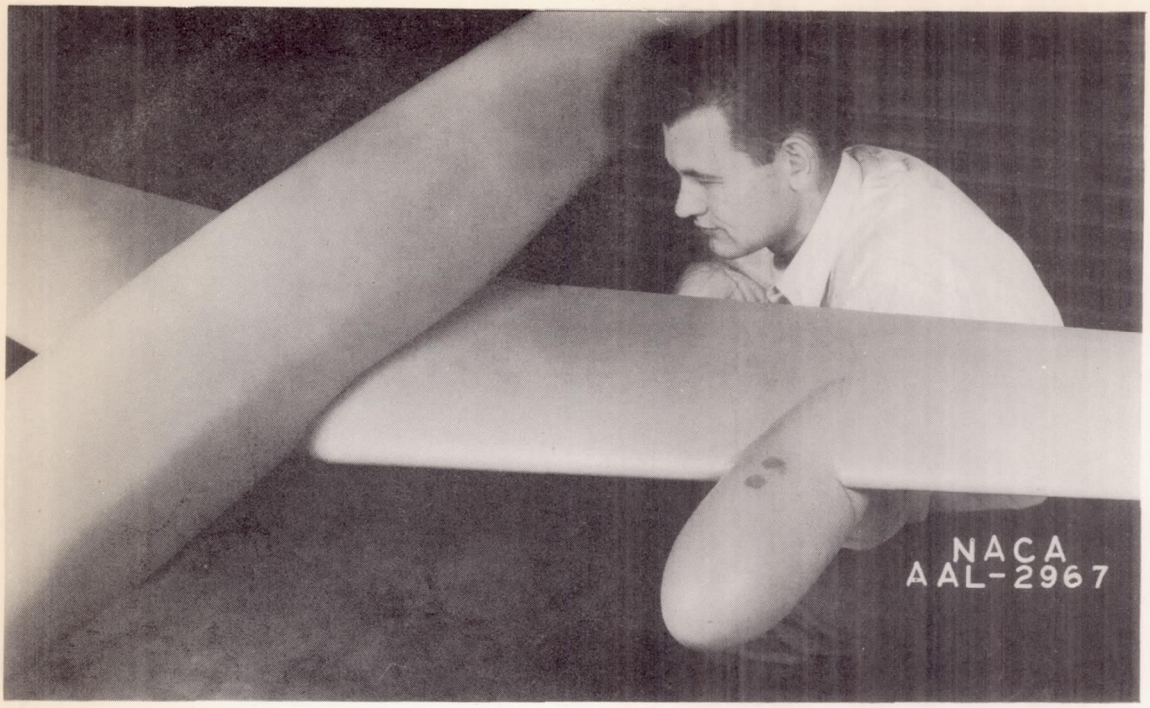

Figure 3.- Details of smooth faired nose on outboard nacelle (outboard nacelles faired).

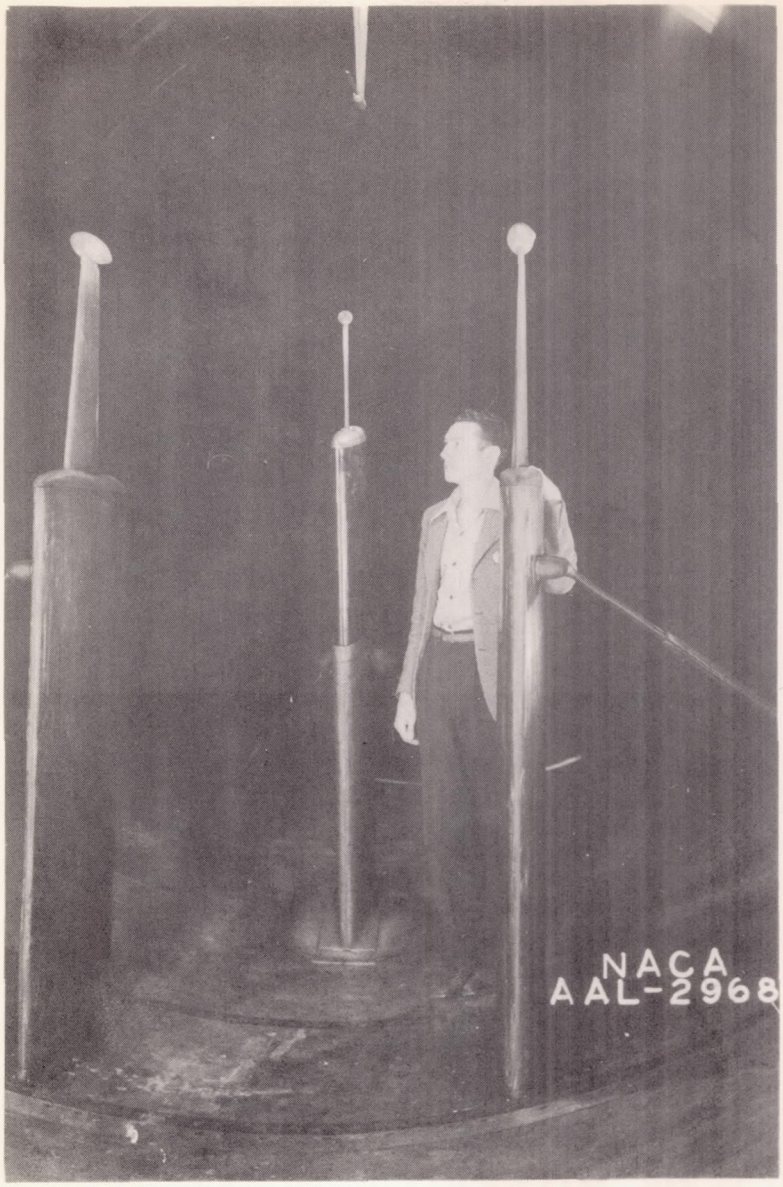

Figure 4.- The tare set up.

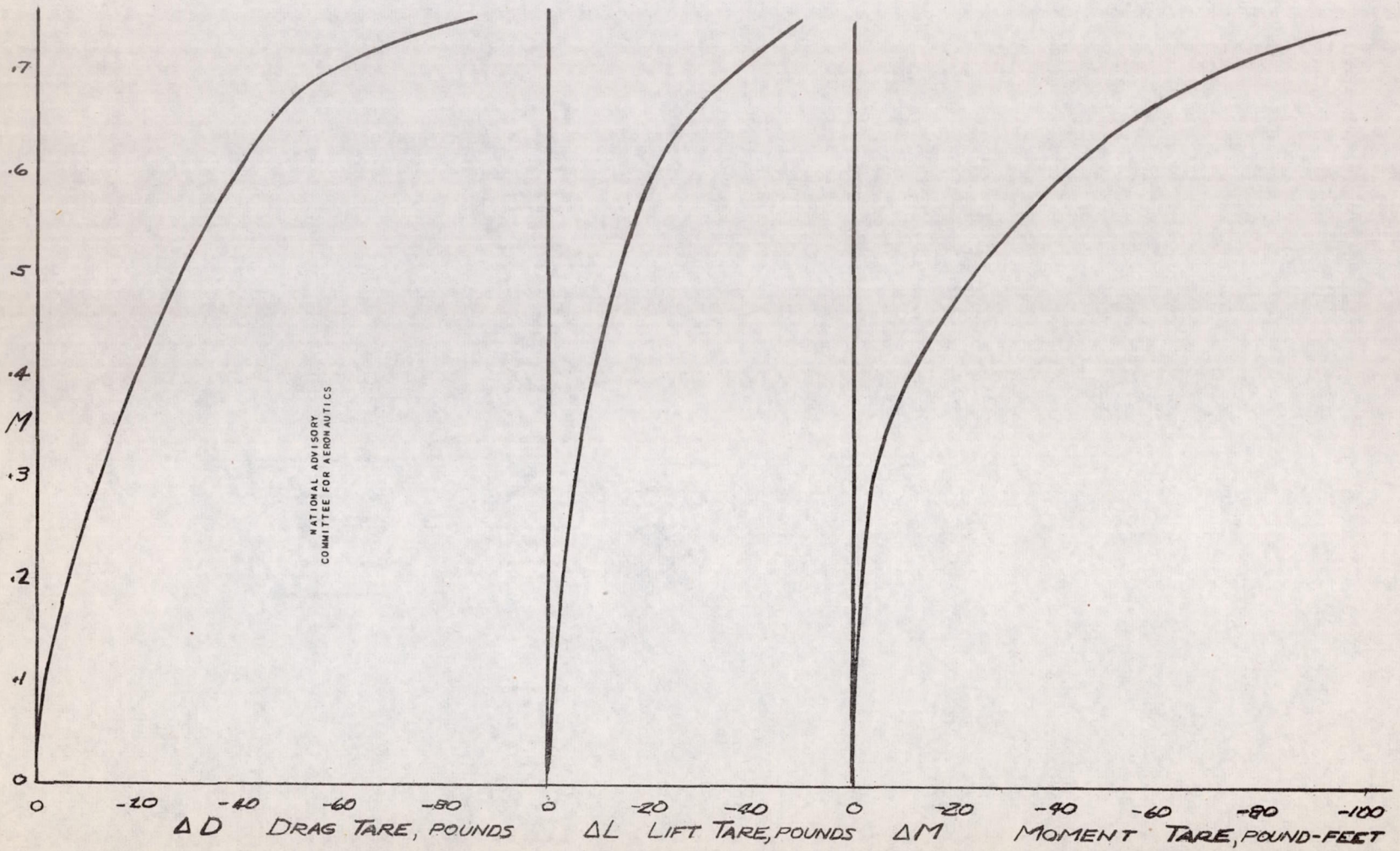

FIGURE 5 STRUT TARES

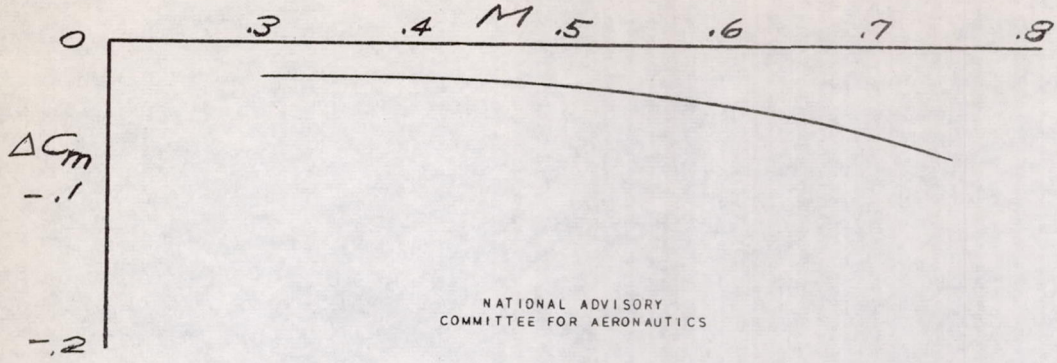

THIS CORRECTION ADDED TO ALL TAIL-ON RUNS

FIGURE 6 MOMENT CORRECTION DUE TO DOWNFLOW AT THE TAIL.

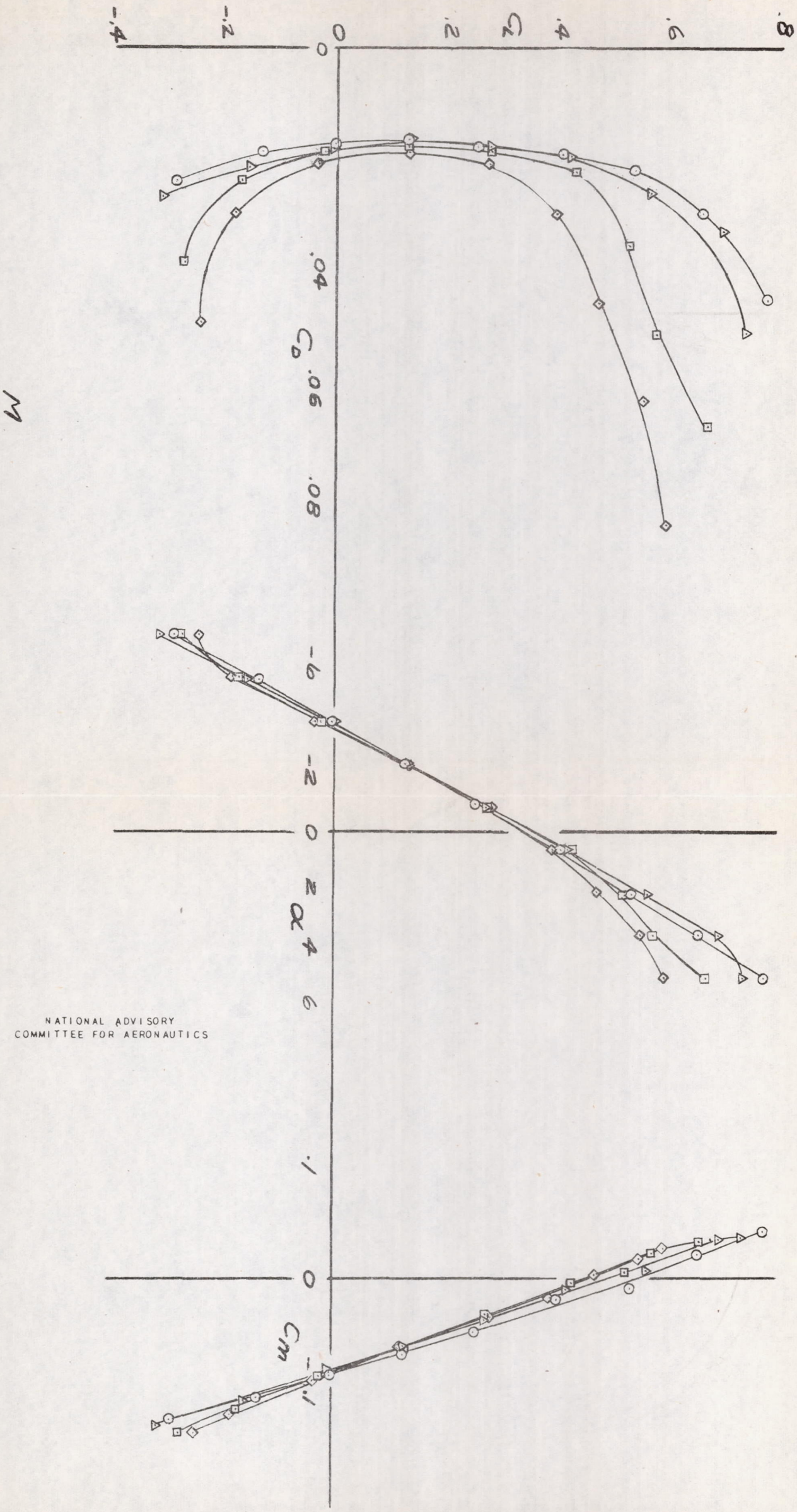

NATIONAL ADVISORY
COMMITTEE FOR AERONAUTICS

FIGURE 7-a WING, FUSELAGE AND OUTBOARD NACELLES FAIRED POLARS AT MACH NUMBERS 0.3, 0.5, 0.6, 0.65

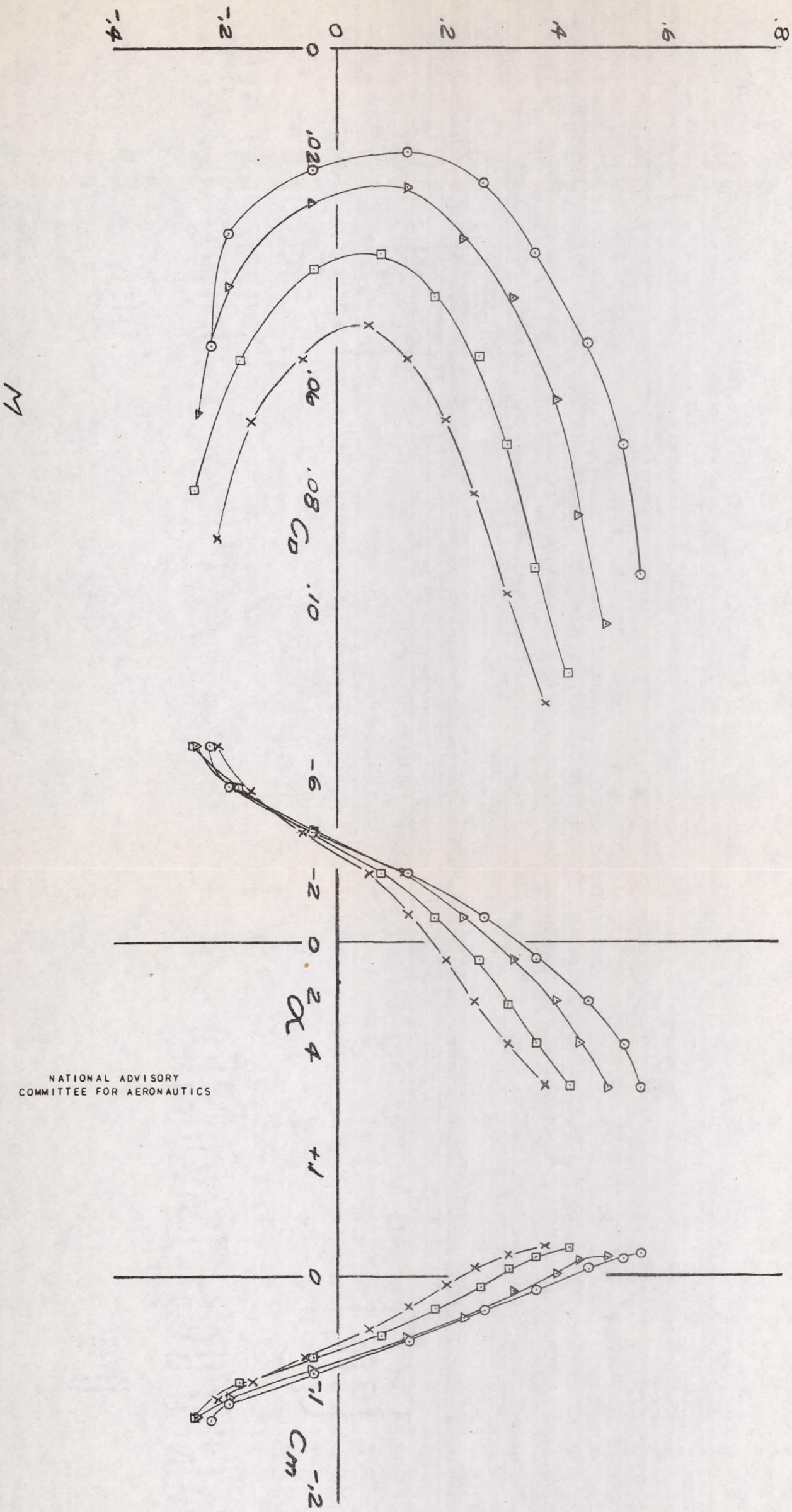

FIGURE 7-b WING, FUSELAGE AND OUTBOARD NACELLES FAIRED. POLARS AT MACH NUMBERS 0.675, 0.7, 0.725, 0.74

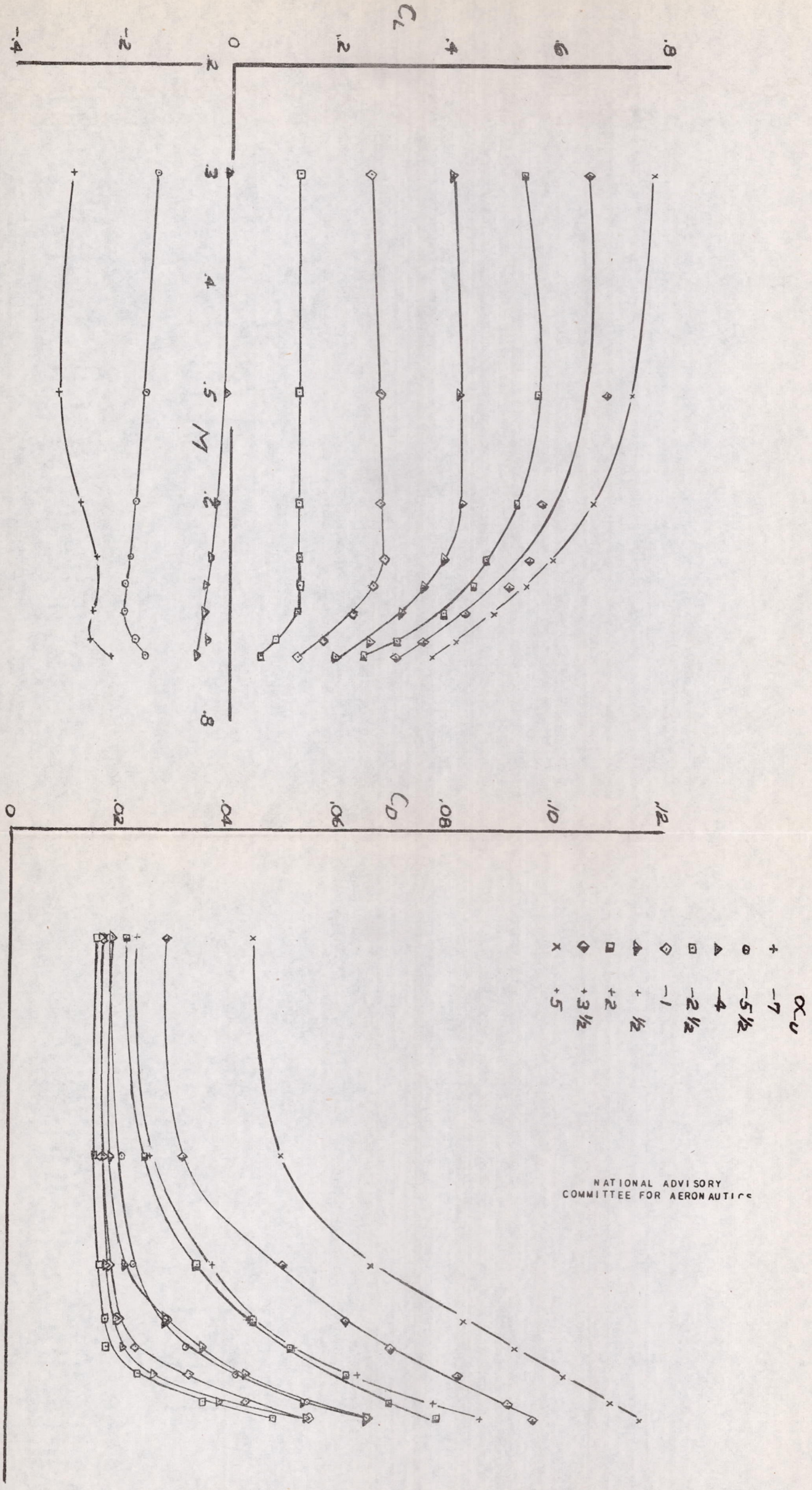

FIGURE 7-C WING, FUSELAGE AND OUTBOARD NACELLES FAIRED.
VARIATION OF C_L AND C_D WITH MACH NUMBER FOR CONSTANT α_u

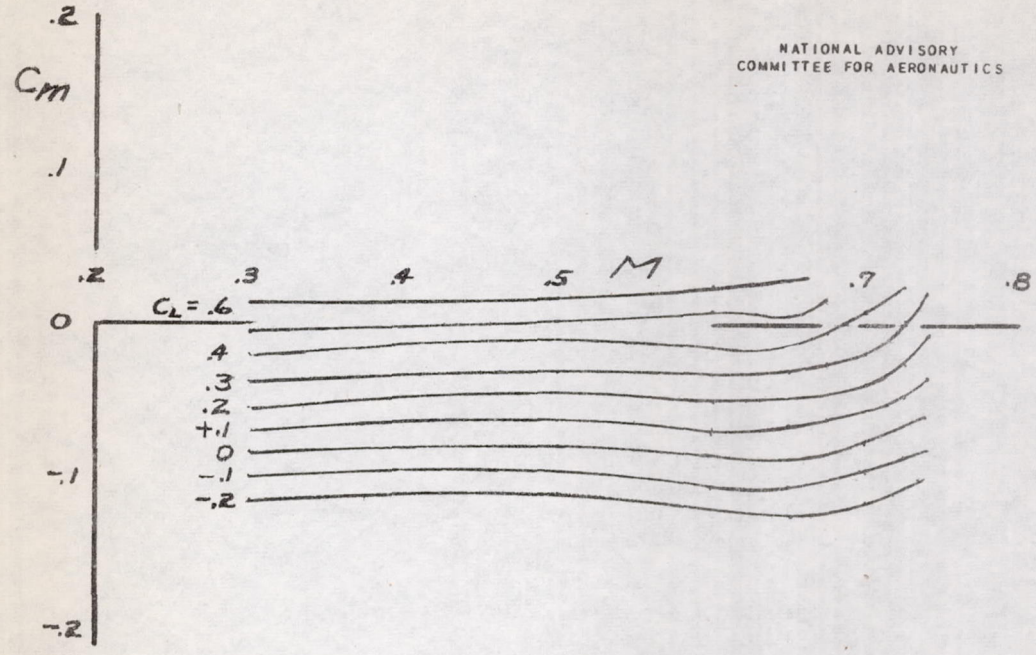

FIGURE 7-d WING, FUSELAGE AND OUTBOARD NACELLES FAIRED. VARIATION OF C_m WITH MACH NUMBER FOR CONSTANT C_L

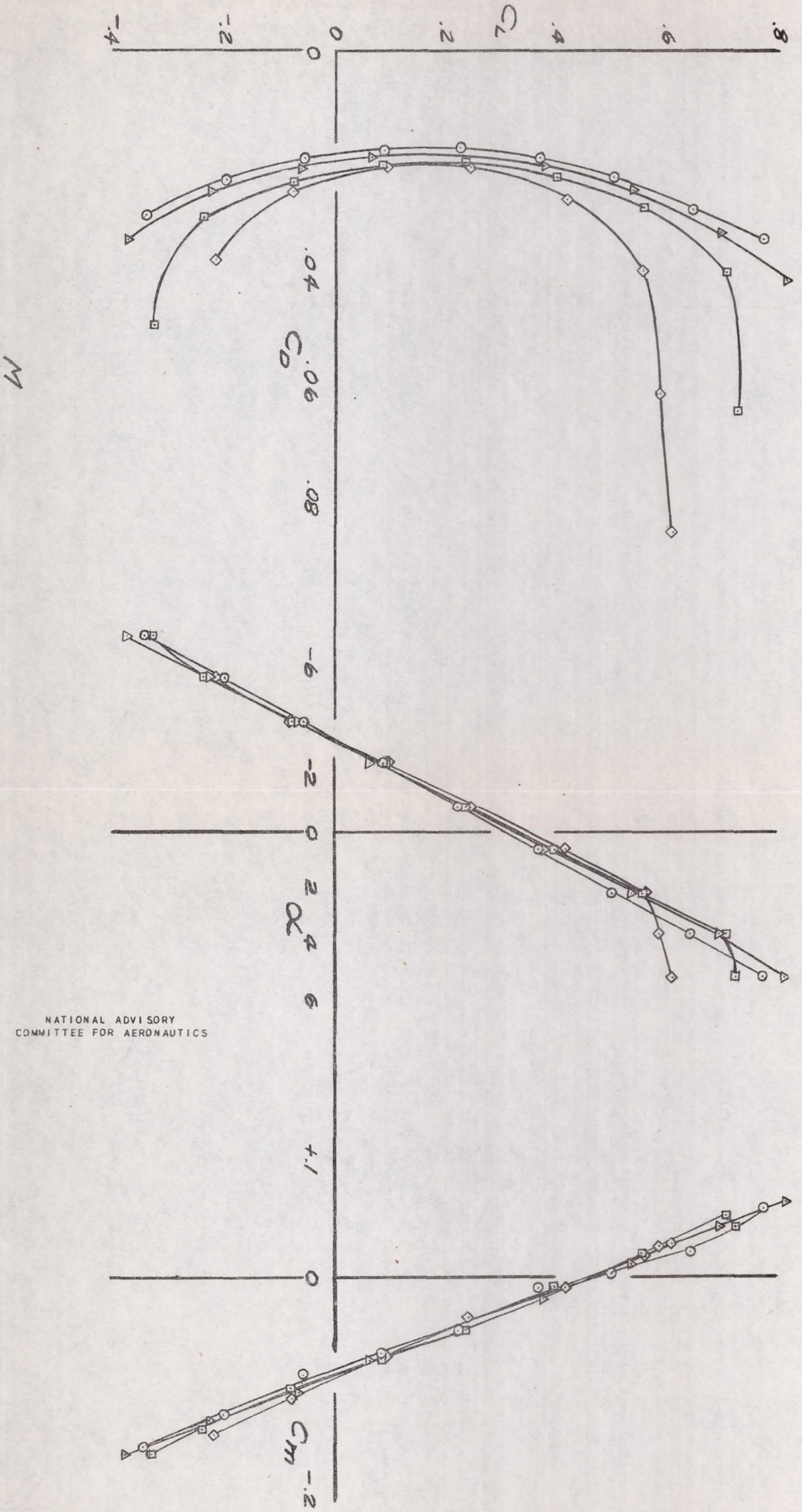

FIGURE 8-a WING, FUSELAGE, FILLETS AND INBOARD AND OUTBOARD NACELLES COWLED POLARS AT MACH NUMBERS 0.3, 0.5, 0.6, 0.65

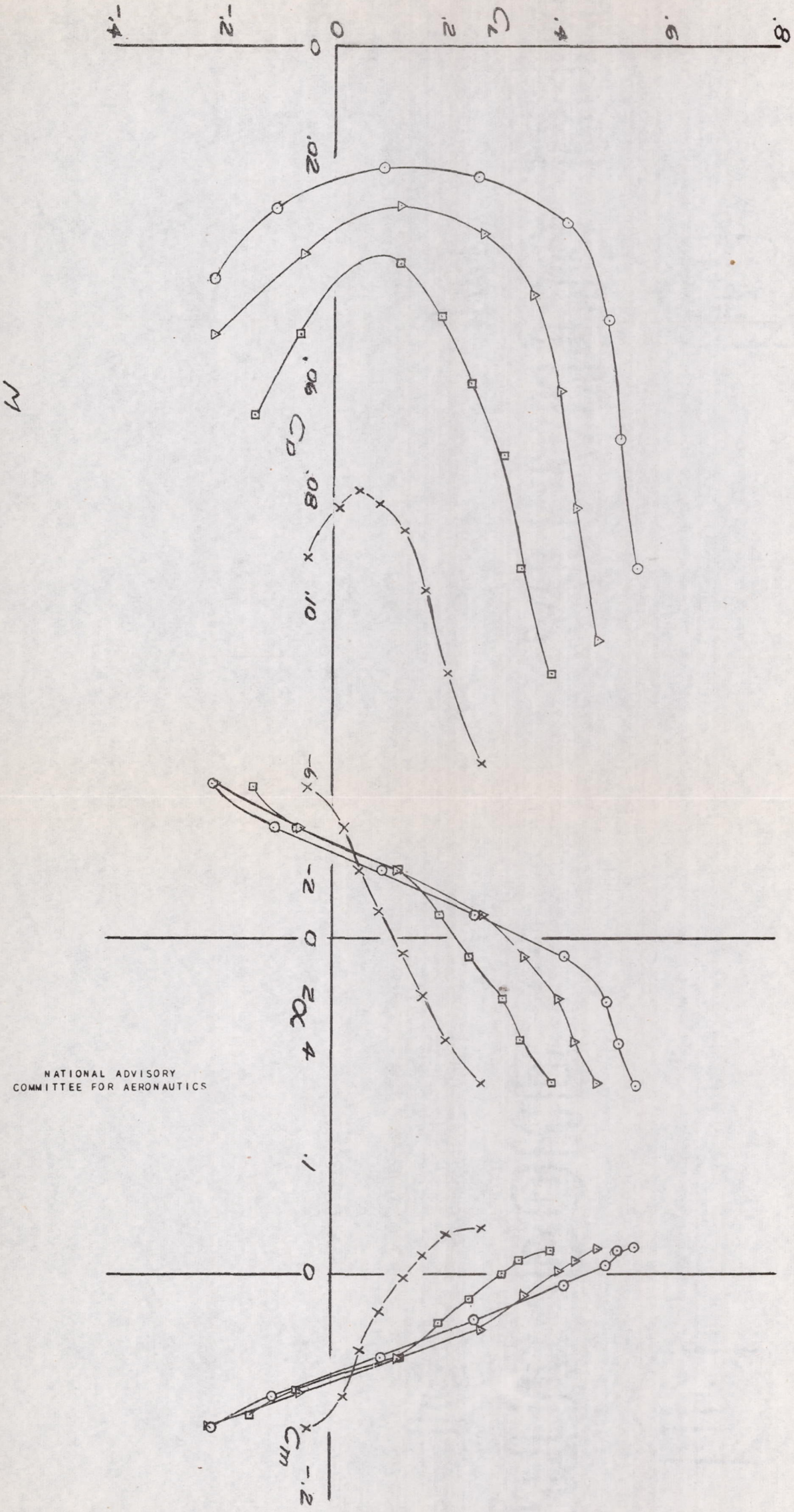

FIGURE 8-b WING, FUSELAGE, FILLETS AND INBOARD AND OUTBOARD NACELLES COWLED. POLARS AT MACH NUMBERS 0.675, 0.7, 0.725, 0.75

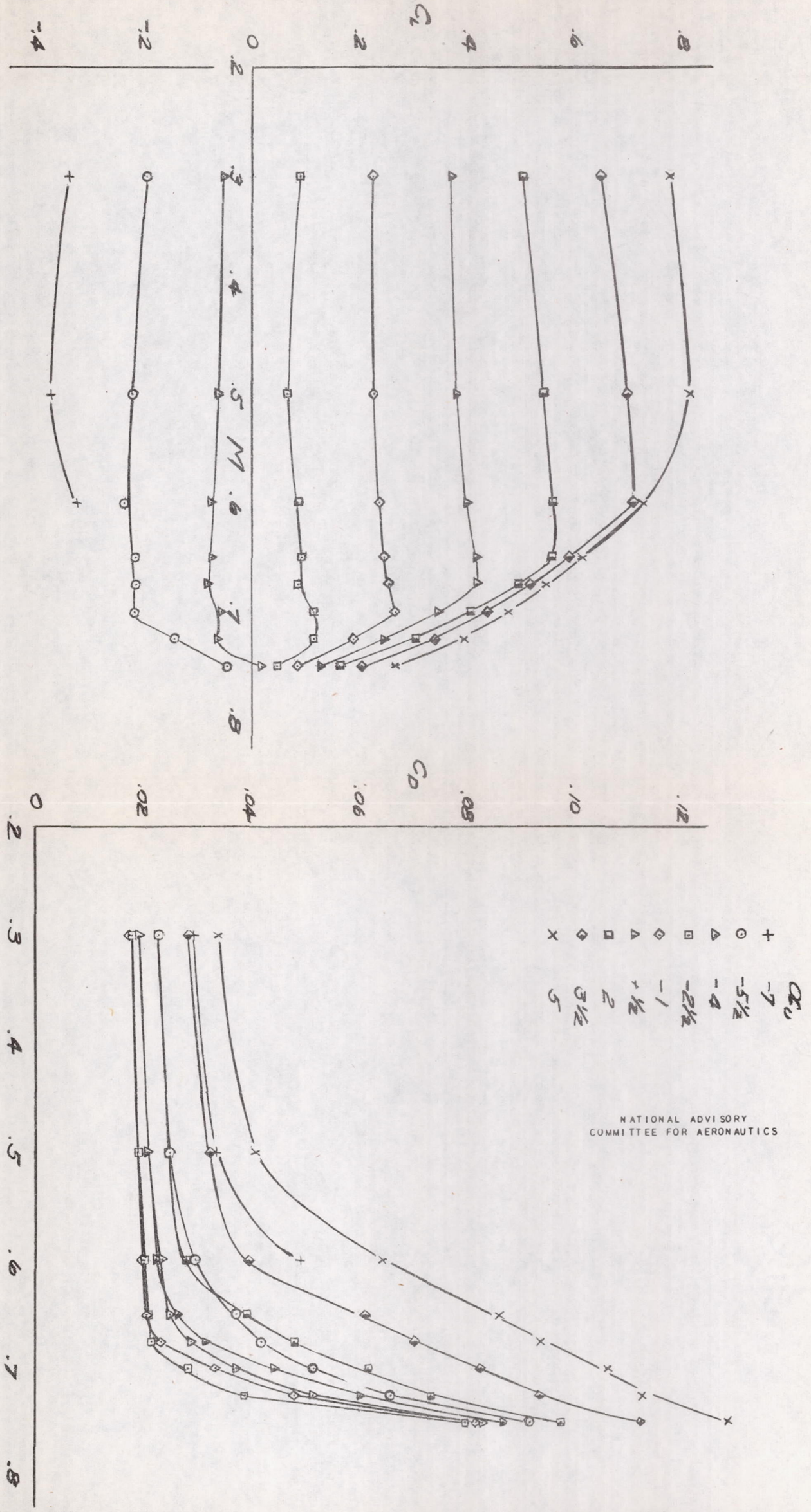

FIGURE 8-C WING, FUSELAGE, FILLET AND INBOARD AND OUTBOARD NACELLES COWLED
VARIATION OF C_L AND C_D WITH MACH NUMBER FOR CONSTANT α_v

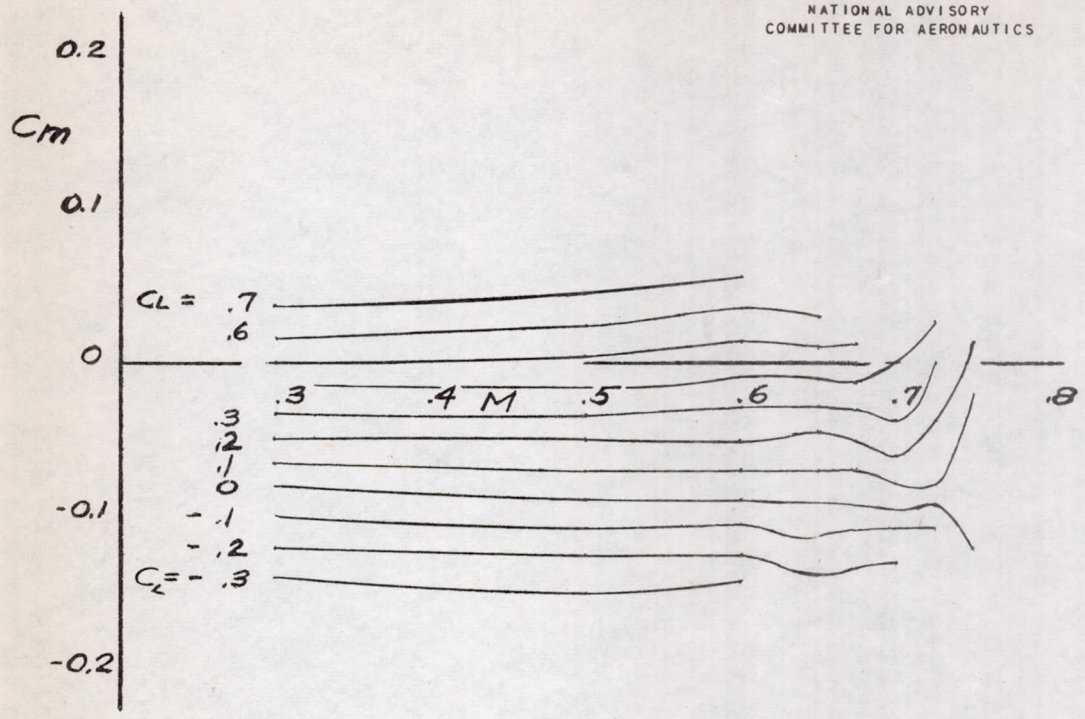

FIGURE 8d WING, FUSELAGE, FILLETS AND INBOARD AND OUTBOARD NACELLES COWLED.
VARIATION OF C_m WITH MACH NUMBER.

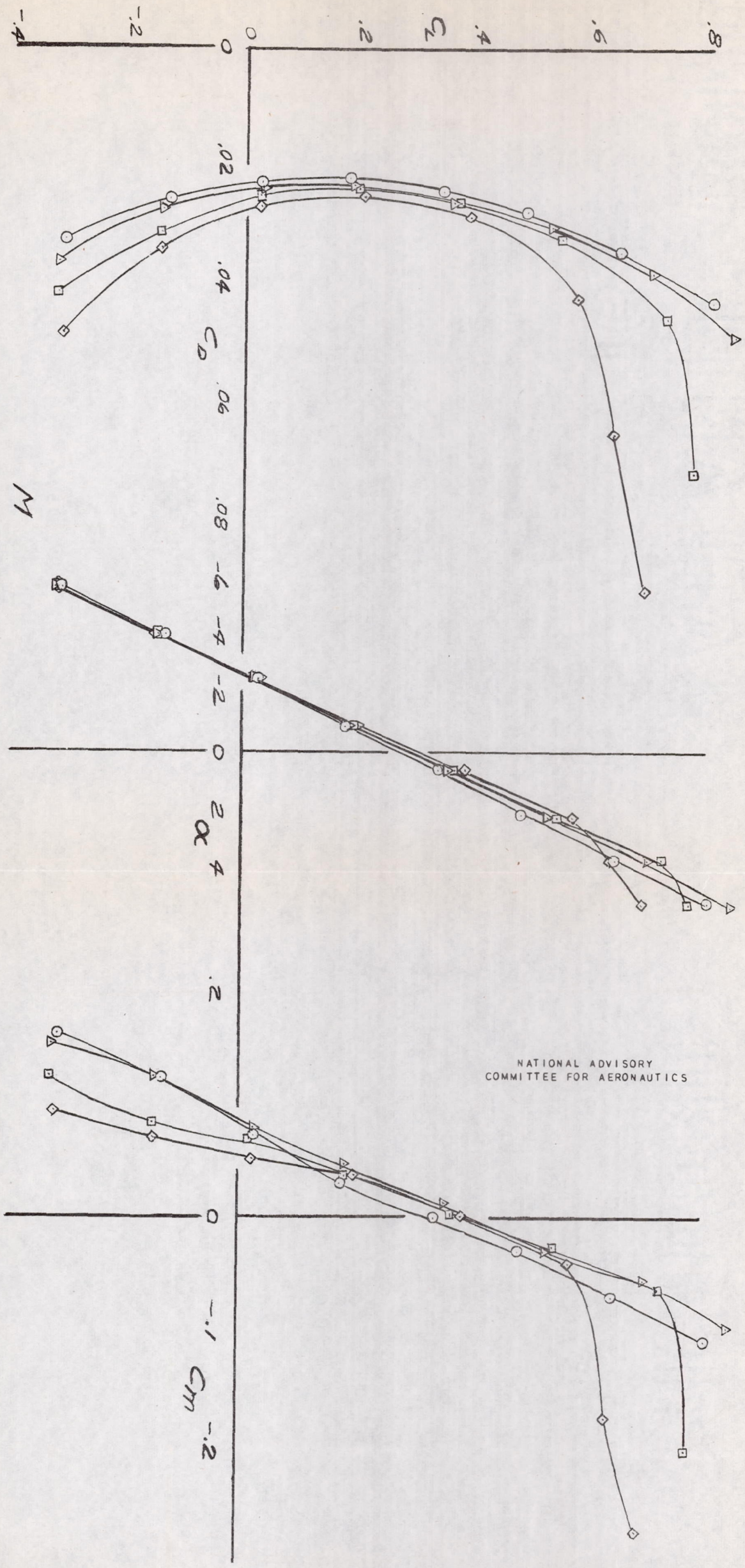

FIGURE 9-a COMPLETE MODEL WITH ELEVATORS AT 0°
POLARS AT MACH NUMBERS 0.3, 0.5, 0.6, 0.65

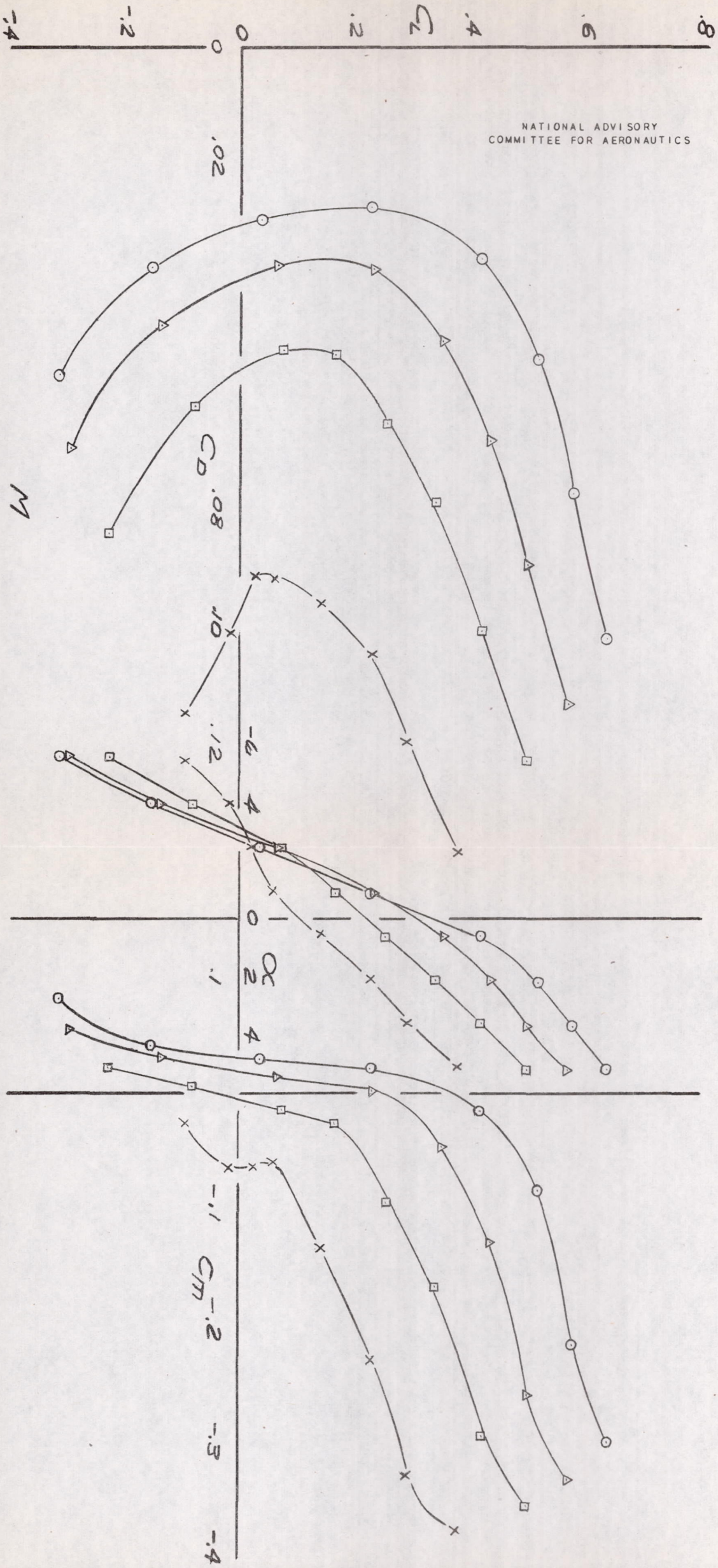

FIGURE 9-b COMPLETE MODEL WITH ELEVATORS AT 0°
POLARS AT MACH NUMBERS 0.675, 0.7, 0.725, 0.75

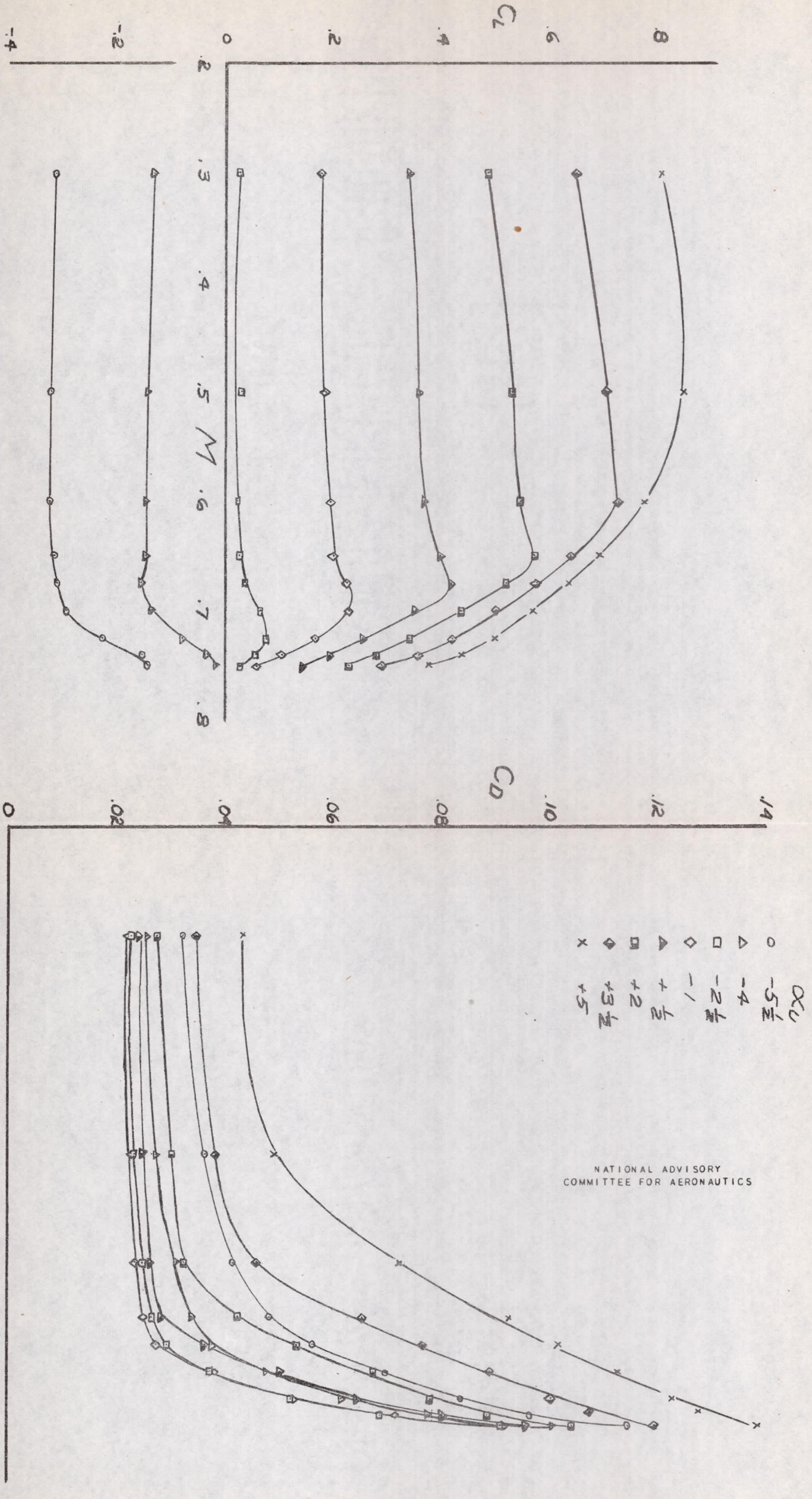

FIGURE 9-c COMPLETE MODEL WITH ELEVATORS AT 0°
VARIATION OF C_L AND C_D WITH MACH NUMBER

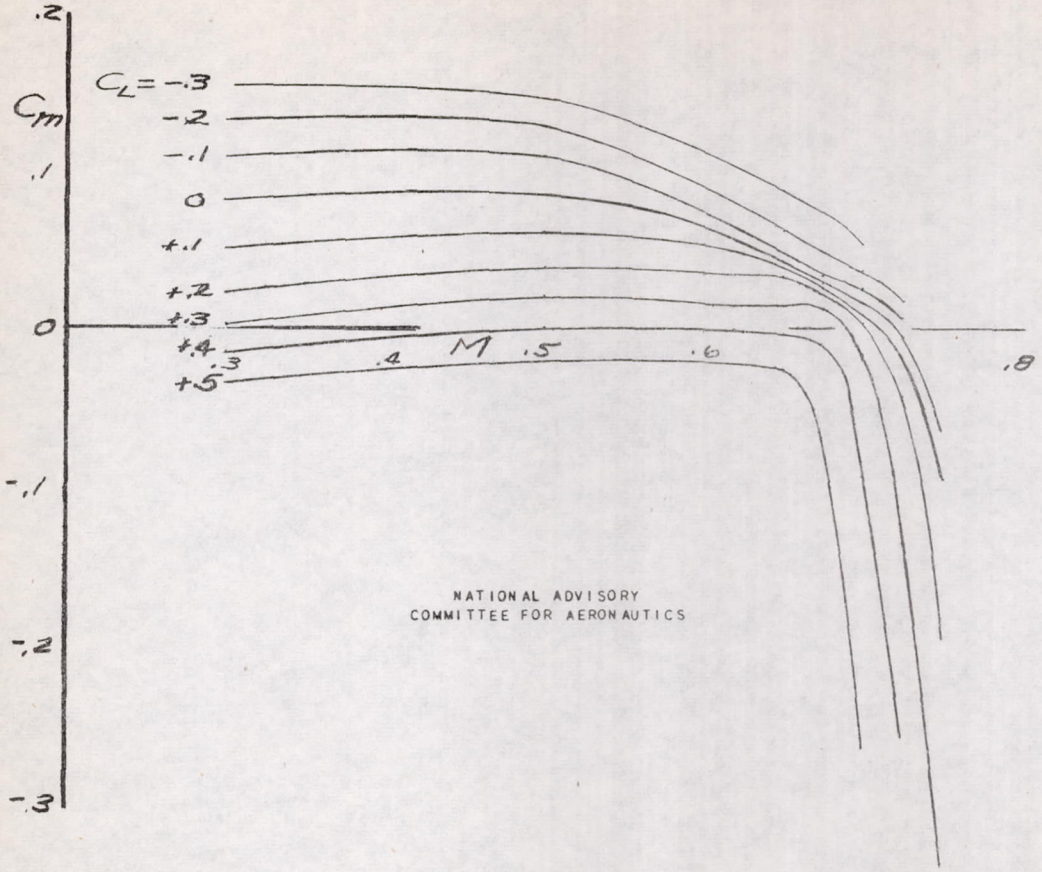

FIGURE 9-d COMPLETE MODEL WITH ELEVATORS AT 0°.
VARIATION OF C_m WITH MACH NUMBER

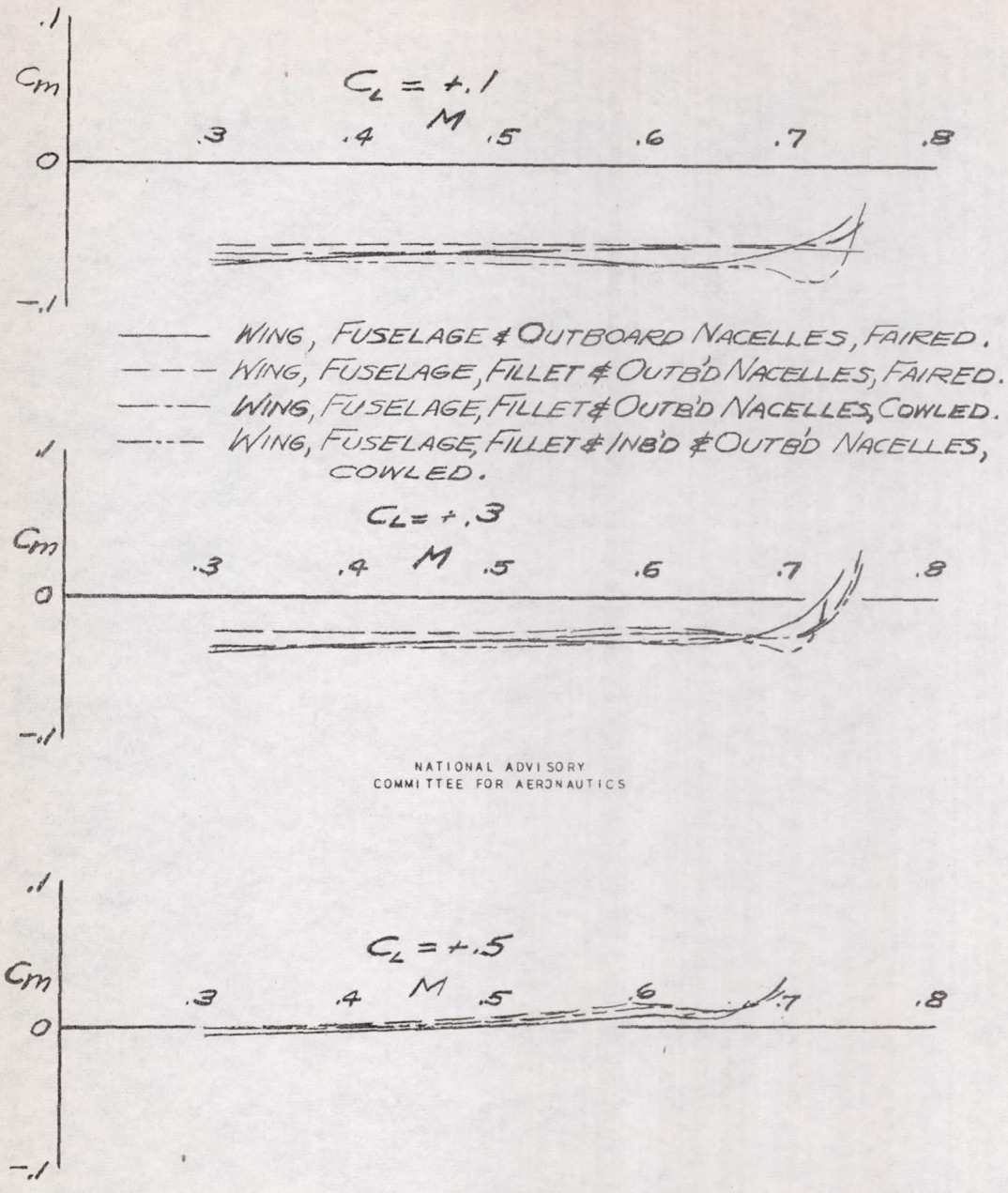

NATIONAL ADVISORY
COMMITTEE FOR AERONAUTICS

FIGURE 10a VARIATION OF C_m WITH MACH NUMBER FOR THE VARIOUS TAIL-OFF CONDITIONS.

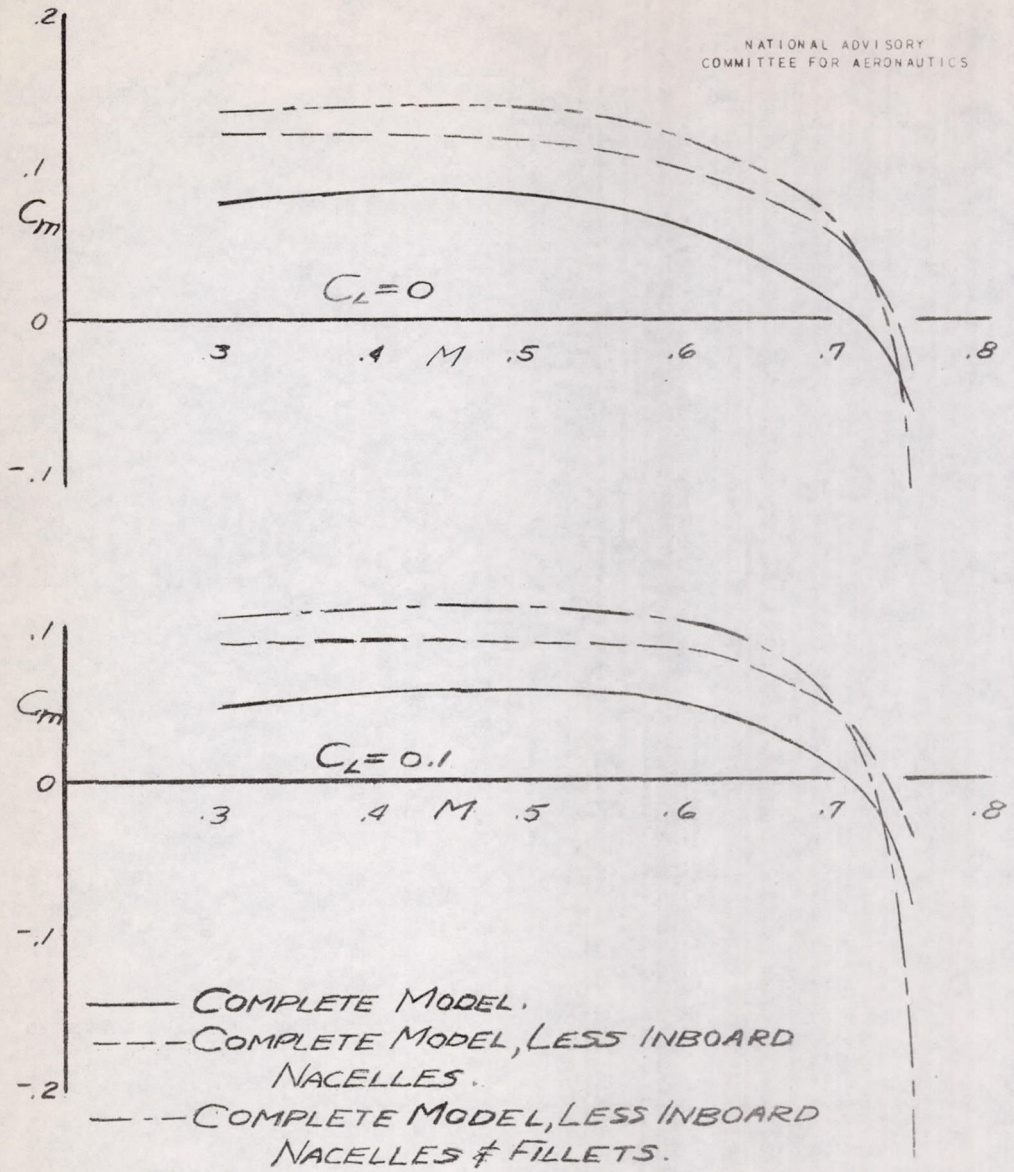

FIGURE 10b VARIATION OF C_m WITH MACH NUMBER FOR THE VARIOUS TAIL-ON CONDITIONS, $C_L = 0$ AND 0.1

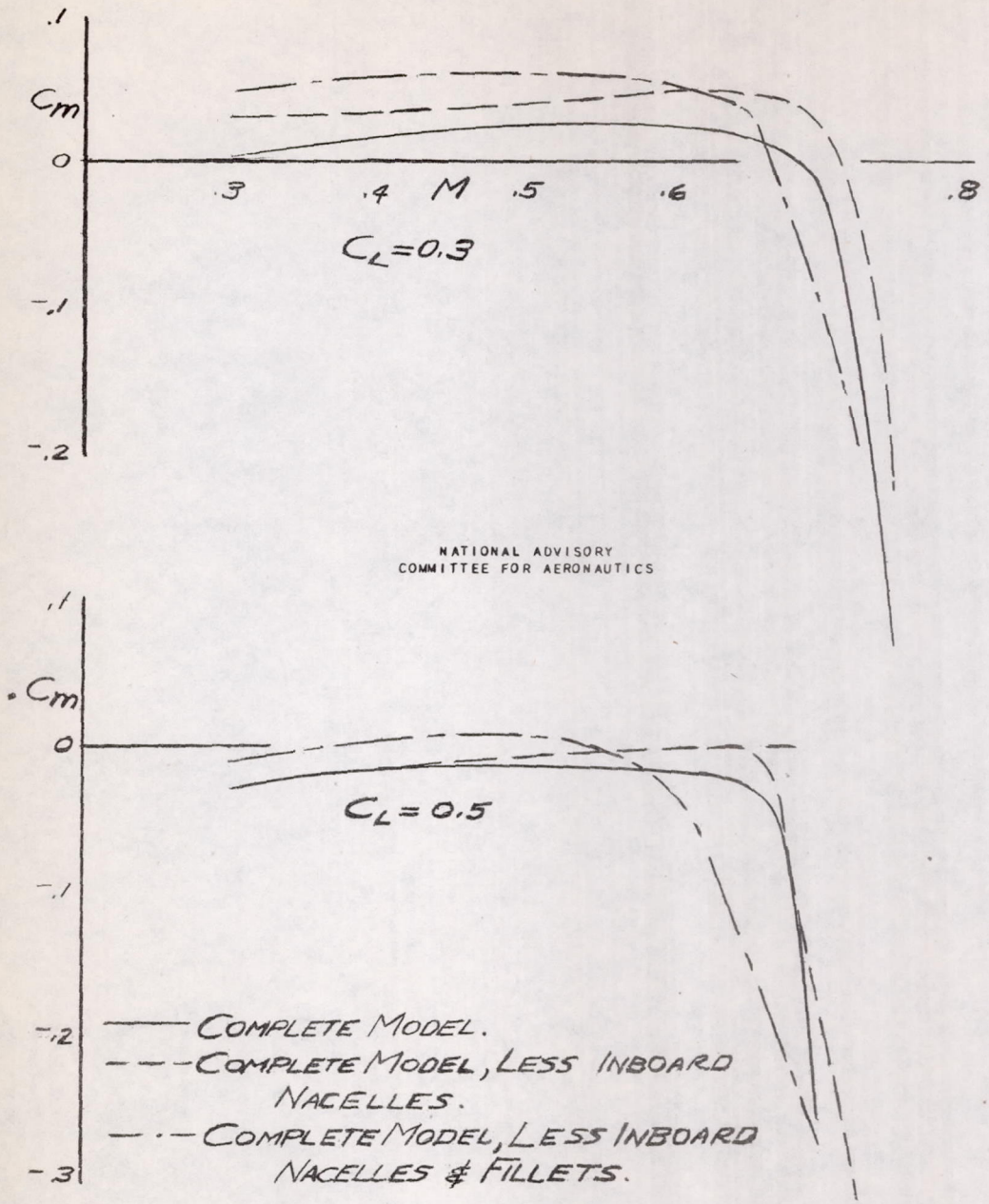

FIGURE 10c VARIATION OF C_m WITH MACH NUMBER FOR THE VARIOUS TAIL-ON CONDITIONS, $C_L = 0.3$ AND 0.5

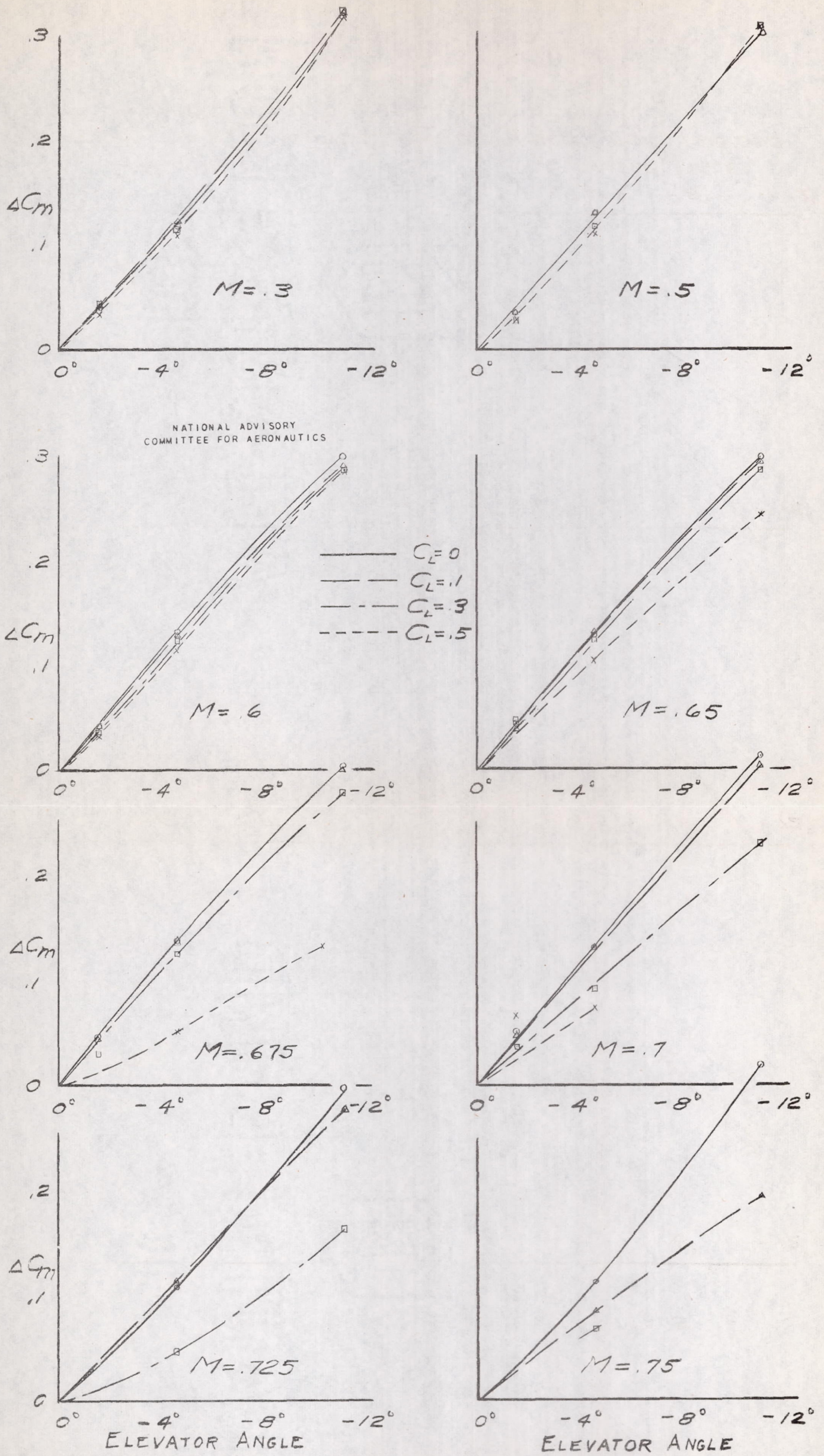

FIGURE 11 VARIATION OF ΔC_m WITH ELEVATOR ANGLE FOR VARIOUS MACH NUMBERS.

KEY

(A) WING, FUSELAGE, & OUTB'D NACELLES FAIRED.
(B) WING, FUSELAGE, FILLET & OUTB'D NACELLES FAIRED.
(C) WING, FUSELAGE, FILLET & OUTB'D NACELLES COWLED.
(D) WING, FUSELAGE, FILLET & INB'D & OUTB'D NACELLES COWLED.
(E) WING, FUSELAGE, TAIL & OUTB'D NACELLES COWLED.
(F) WING, FUSELAGE, FILLET, TAIL & OUTB'D NACELLES COWLED.
(G) COMPLETE MODEL

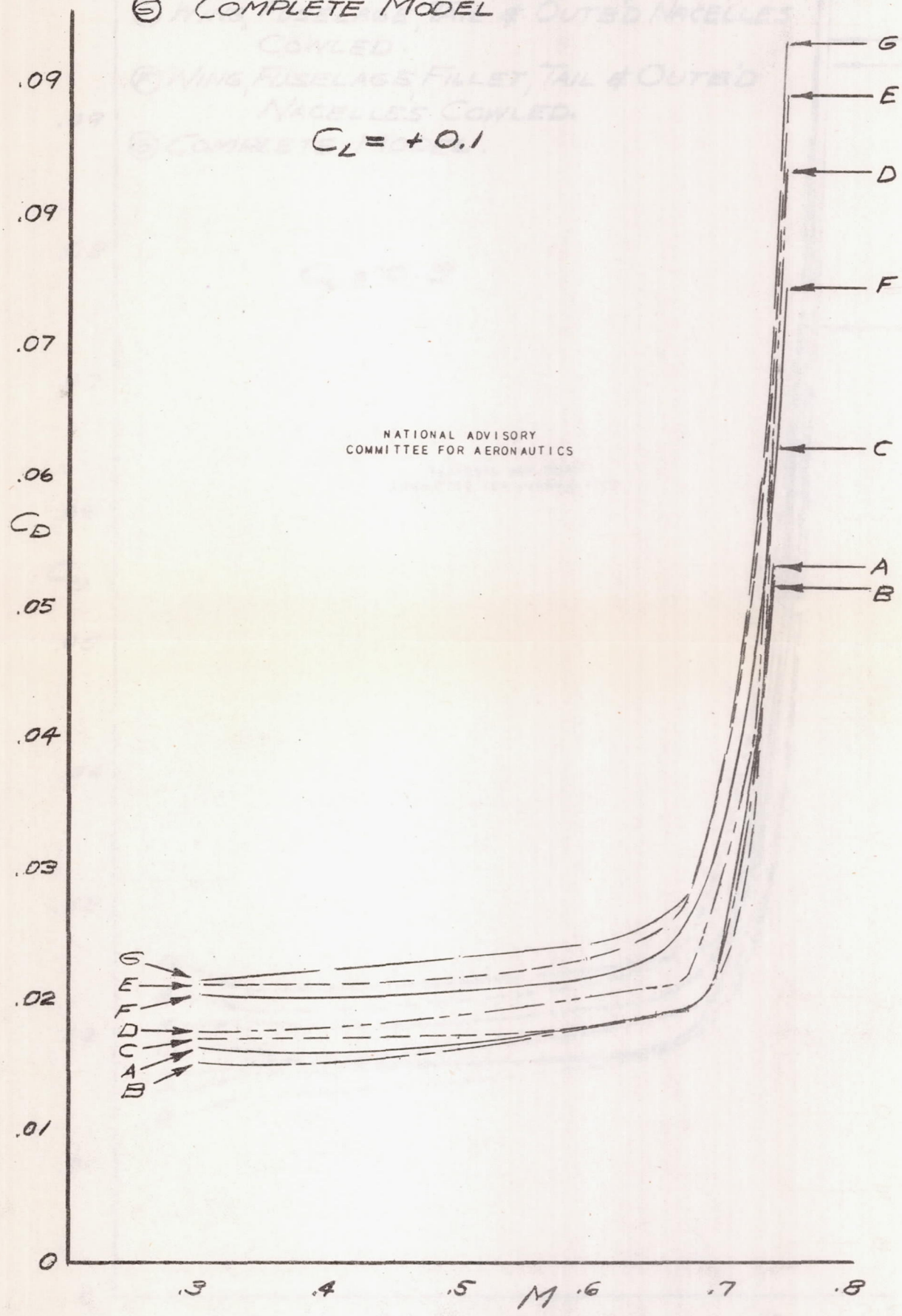

FIGURE 12a VARIATION OF C_D WITH MACH NUMBER FOR THE VARIOUS MODEL CONDITIONS, $C_L = 0.1$

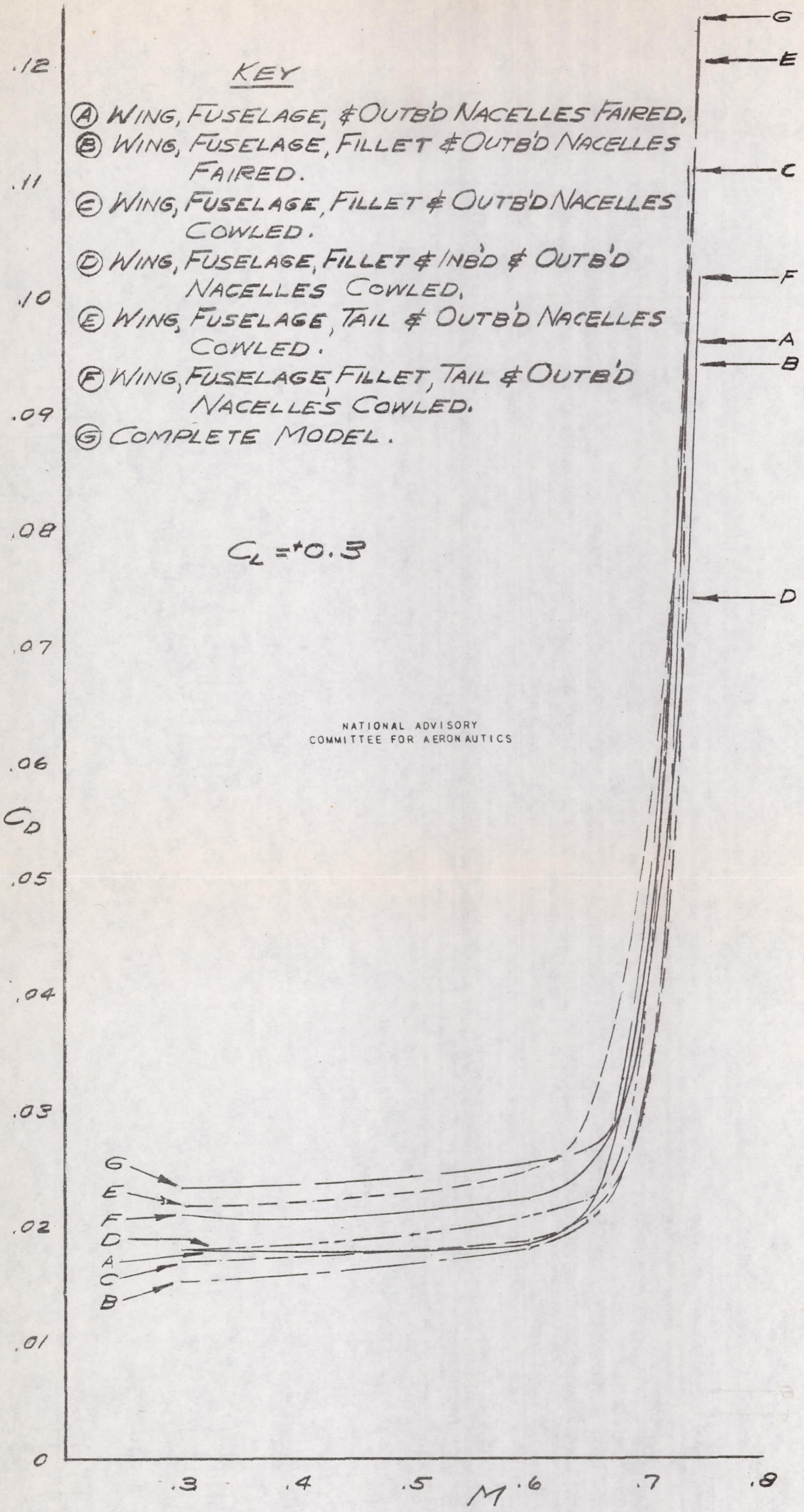

FIGURE 126 VARIATION OF C_D WITH MACH NUMBER FOR THE VARIOUS MODEL CONDITIONS, $C_L = 0.3$

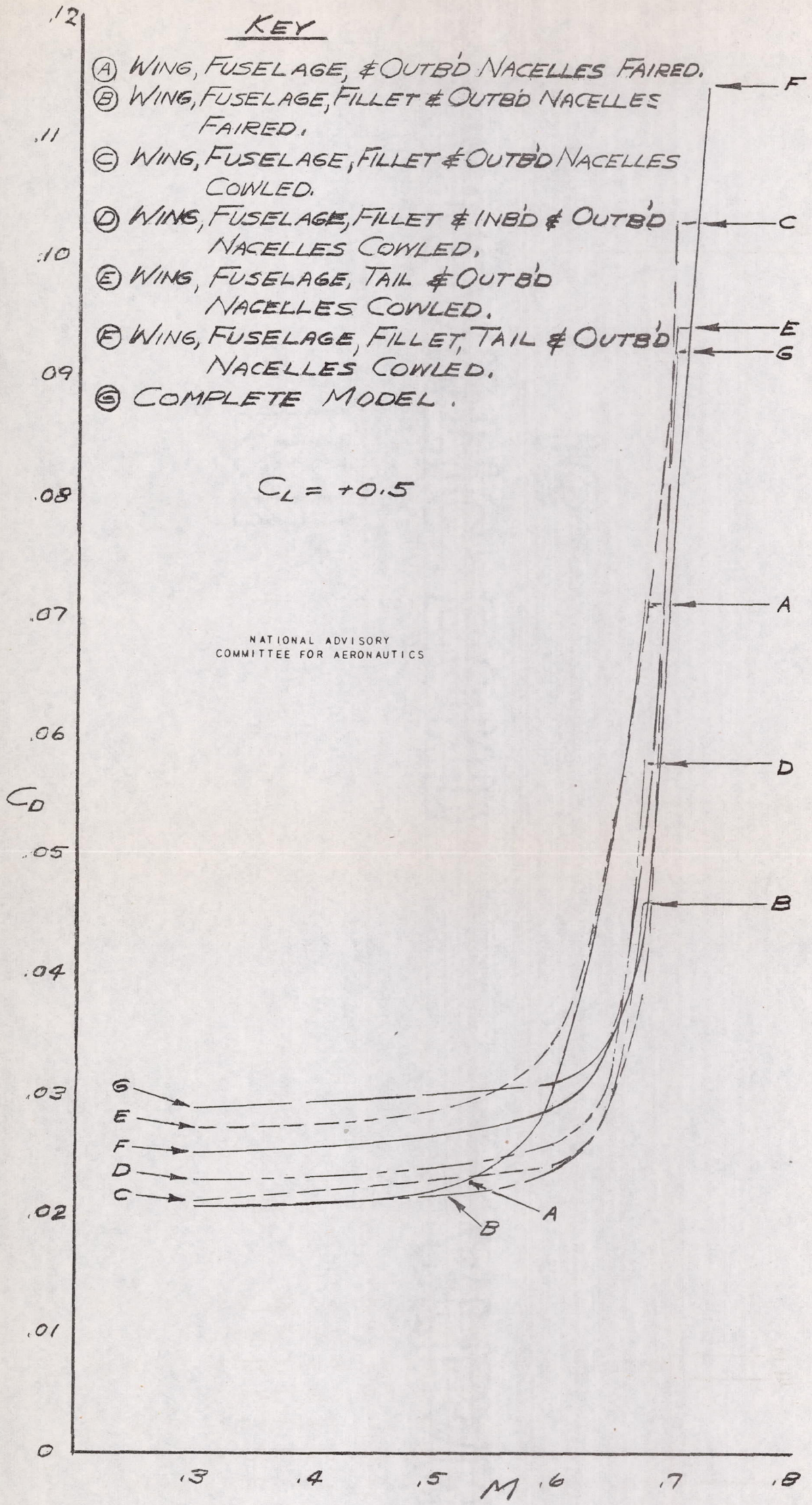

FIGURE 12c VARIATION OF C_D WITH MACH NUMBER FOR THE VARIOUS MODEL CONDITIONS, $C_L = 0.5$